

# SCRUTINIZING BARREMIAN COPROLITE INCLUSIONS TO RECORD DIGESTIVE STRATEGIES

Sandra BARRIOS-DE PEDRO & Ángela D. BUSCALIONI

*Departamento de Biología (Paleontología) and Centro para la Integración en Paleobiología (CIPb),  
Universidad Autónoma de Madrid, Cantoblanco 28049 Madrid, Spain;  
e-mails: [sandra.barrios@uam.es](mailto:sandra.barrios@uam.es); [angela.delgado@uam.es](mailto:angela.delgado@uam.es)*

Barrios-de Pedro, S. & Buscalioni, D. Á., 2018. Scrutinizing Barremian coprolite inclusions to record digestive strategies, *Annales Societatis Geologorum Poloniae*, 88: 20–221.

**Abstract:** The exceptional preservation of the Las Hoyas coprolites allows the taphonomic study of inclusions on twelve morphotypes and twenty-three specimens. Non-destructive techniques were applied to study the digestion features (pitting, corrosion lines, shape of the fractures at the ends) and the arrangement, number, and size of inclusions. An analysis based on non-metric, multidimensional scaling ordination identified the similarities among the inclusion features and morphotypes. The morphotypes are clustered on the basis of the way of ingestion and the digestive process. The authors recognize three digestive strategies for the Las Hoyas coprolites: (1) ingestion of prey with limited processing in the mouth, scarce to less effective acid secretions, and/or defecation in a short period of time; (2) ingestion of the prey with mastication prior to deglutition, and defecation over a longer period of time; (3) mastication and long retention time of food in the digestive system with more effective acid secretions. This study is a first step in the understanding of the feeding ecology of the Las Hoyas Barremian lentic ecosystem, based on coprolites.

**Key words:** Cretaceous, Las Hoyas, lacustrine, taphonomy, digestive process, feeding ecology.

*Manuscript received 19 April 2018, accepted 19 October 2018*

## INTRODUCTION

Las Hoyas is an upper-Barremian continental Konservat-Lagerstätte located in Cuenca, central Spain, that has yielded a vast diversity of plant and animal body fossils and ichnofossils (Buscalioni and Poyato-Ariza, 2016). Coprolites are among the most abundant remains, with almost 2,000 coprolites collected. A total of twelve different coprolite morphotypes have been described: spiral, circular, irregular, elongated, rosary, ellipsoidal, cylinder, bump-headed lace, fir-tree, cone, straight lace, and thin lace coprolites (Barrios-de Pedro *et al.*, 2018a). The Las Hoyas ichnoassemblage contains not only an exceptional diversity of coprolite morphologies, but also provides the opportunity to explore the taphonomy of inclusions and infer the digestive strategies of the coprolite producers. Most of the rich Mesozoic coprolite assemblages are from marine and transitional environments (e.g., Eriksson *et al.*, 2011; Niedźwiedzki *et al.*, 2016; Luo *et al.*, 2017), while the Las Hoyas coprolite association was produced in a lacustrine carbonate environment, interpreted as a stationary, subtropical, inland wetland, dominated by periphyton and microbial mats (Fregenal-Martínez and Meléndez, 2016; Fregenal-Martínez *et al.*, 2017). Therefore, bacterial sealing has been proposed as one of the most influential processes behind the exceptional preservation at

Las Hoyas (Buscalioni and Fregenal-Martínez, 2010; Iniesto *et al.*, 2013, 2016; Guerrero *et al.*, 2016), contributing decisively to the protection of the coprolite inclusions.

In a previous contribution, a dichotomous key to delimit the Las Hoyas coprolite morphotypes was elaborated, indicating that these coprolites mostly correspond to carnivorous producers with ichthyophagous diets, such as crocodiles, urodelaans and different kind of fishes (Barrios-de Pedro *et al.*, 2018a). The aim of this paper is to describe and determine the taphonomic properties of the inclusions contained in the Las Hoyas coprolites; these properties were studied for each morphotype. The combination of such properties in every morphotype is discussed to differentiate the patterns of digestive processes and infer some of the digestive strategies of the producers. In general, this study aims to explore the patterns of digestive strategies to extrapolate which was the most dominant in this Barremian ecosystem. The digestive strategies are reflected in the abundance of undigested food and the lines of evidence left by digestive processes, such as fermentation and enzymatic degradation (see Stevens and Hume, 1995; Furness *et al.*, 2015). Because digestive strategies can be shared by different groups (e.g., fish and amphibians), the present authors here evaluate the cor-

relation between morphotypes and inclusions, rather than morphotypes and producers (Hunt *et al.*, 2012). This study is the first step towards understanding the feeding ecology of the Las Hoyas continental Barremian wetland.

## GEOLOGICAL SETTING

The Las Hoyas fossil site is a Konservat-Lagerstätte in the La Huérguina Formation (upper Barremian). It is located in the Serranía de Cuenca (east-central Spain; Fig. 1), which is part of the Iberian Range. This locality consists of finely laminated limestones, composed almost entirely of calcium carbonate (Fregenal-Martínez and Meléndez, 2016; Fregenal-Martínez *et al.*, 2017). The currently accepted depositional model for the laminated facies of Las Hoyas distinguishes two groups of facies associations (Buscalioni and Fregenal-Martínez, 2010). One association type would have been deposited during wetter periods by traction or suspension fallout of allochthonous carbonate, while the other type would have been formed by the autochthonous production of carbonate, linked to the growth of microbial mats during drier periods of a low water column. The alternation of both associations is related to a seasonal, subtropical habitat with a regional climate, alternating between wet and dry seasons (Fregenal-Martínez and Meléndez, 2016). The depositional system corresponds to a continental sedimentary environment, in which Las Hoyas would have been a shallow lake, being part of an inland freshwater system of wetlands on a regional scale (Poyato-Ariza *et al.*, 1998; Bailleul *et al.*, 2011, Fregenal-Martínez *et al.*, 2017). This scenario explains the coexistence of terrestrial and aquatic organisms and traces.

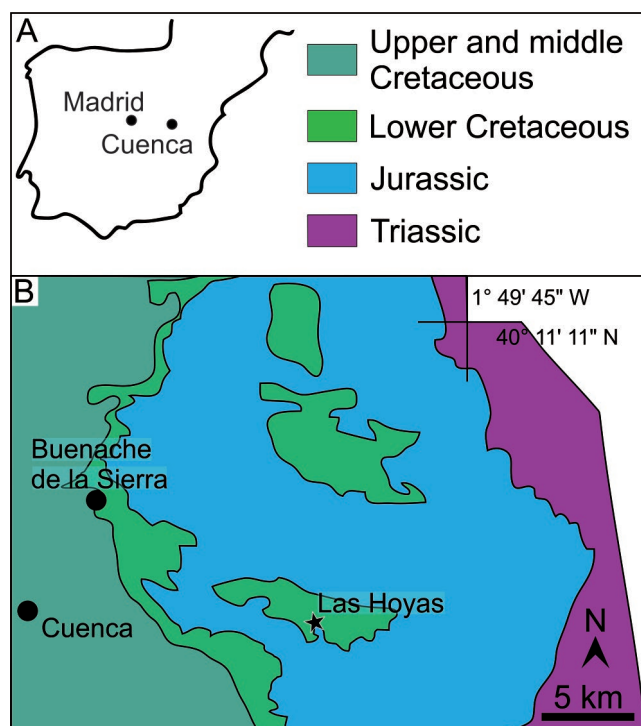


**Fig. 1.** Location maps. **A.** Simplified map of the Iberian Peninsula showing the location of Cuenca. **B.** Simplified geological map of the Las Hoyas area.

## The Las Hoyas ichnoassemblage

The ichnoassemblage is characterized by the aquatic *Mermia* ichnofacies, which at Las Hoyas shows limited diversity of invertebrate aquatic traces. The locality also contains vertebrate terrestrial footprints (Buatois *et al.*, 2000; Gibert *et al.*, 2016). The aquatic trace fossils consist of very shallow-tiered, endogenic, invertebrate burrows and trails, restricted to some bedding planes. The deposit exhibits minor effects of bioturbation, favouring the exceptional preservation of the finely laminated, primary sedimentary fabric. Therefore, the poor and shallow *Mermia* ichnofacies confirms that the substrate was highly stressed by the limited availability of oxygen and anoxia would have been a key factor in promoting the exquisite preservation of fossils, together with bacterial sealing (Buscalioni and Fregenal-Martínez 2010).

## METHODS AND MATERIALS

### Materials

The coprolites studied are housed at the Museo de las Ciencias de Castilla-La Mancha (MCCM) and belong to the Las Hoyas (LH) collection. A summary of the main characteristics for the twelve morphotypes described in Barrios-de Pedro *et al.* (2018a) is provided in Table 1. Every morphotype was subsumed into the morphological classification of faeces, which also includes the producers, provided by Hunt and Lucas (2012, see Table 1).

Most of the Las Hoyas coprolites are preserved in part and counterpart. Each slab is identified by the letters 'a' or 'b' after the specimen number. Specimen numbers not followed by letters correspond to unsplit specimens (i.e., specimens that are whole). Mostly, coprolites expose a section characterized by two linear dimensions (length and diameter, see Table 2). The surface of these sections is irregularly shaped, and different levels of coprolite matrix are exposed. The diameter ranges were categorized in the following states: 1 =  $\leq 5$  mm; 2 = 5–9.9 mm; 3 = 10–19.9 mm; 4 =  $\geq 20$  mm.

### Techniques

In order to explore the inclusions in the coprolite matrix, non-destructive techniques were employed. Macro-scale photos of coprolites were taken, using a D5100 Nikon Reflex camera at the Biology Department of Universidad Autónoma de Madrid (UAM). Other techniques, such as Scanning Electron Microscope (SEM) analyses with a low-vacuum Environmental Scanning Electron Microscope (ESEM\_QUANTA200) and a 3D high-resolution microscope with interferometric and profilometry (Leica DCM8) were carried out at the Museo Nacional de Ciencias Naturales (MNCN) in Madrid. The ImageJ software (Fiji) was used for measurements (Rasband, 1997–2018).

### Criteria and features

A set of features of the inclusions were obtained to infer the digestive strategies characterizing the Las Hoyas co-

proliferation association. The digestive strategies are discussed following the criteria used for the 'gut-reactor' digestion model (Penry and Jumars, 1987; Stevens and Hume, 1995; Furness *et al.*, 2015). The gut-reactor model combines the gut architecture, gut capacity, intake level, dietary composition, digesta passage rate, and digestion rate (Penry and Jumars, 1987). Therefore, in order to integrate such parameters to discuss the digestive strategy, the following variables were explored in a comprehensive manner (see Table 2): (1) the abundance of undigested food, in order to estimate the intake level; (2) the identification of inclusions, in order to evaluate the dietary composition; (3) the size of inclusions and (4) the arrangement of inclusions in the coprolite matrix, in order to discuss digesta and digestion rates; and finally (5) some features related to the digestive process, in order to obtain some values related to the chemical process (Fernández-Jalvo and Andrews, 2016).

- 1) Number of inclusions. The counting of remains was performed from photographs at the macroscale and the visible inclusions in every coprolite were categorized into four states (1,  $N < 15$ ; 2,  $N = 15-30$ ; 3,  $N = 31-45$  and 4,  $N > 45$ ). The smallest remains would correspond on average to 0.2 mm; those observed with SEM analyses were not taken into account for these data.
- 2) Identification of inclusions. When possible, inclusions were identified considering their nature, their anatomical elements and/or their taxonomy. An initial identification was done at the macroscale with a magnifier and SEM then was used to determine the external structures.
- 3) Size of inclusions. The total length of the coprolites, their maximum diameter, and data on the size of their inclusions are given in millimetres (mm). The scale bars of the SEM analyses are provided in microns ( $\mu\text{m}$ ). If the number of inclusions in a coprolite was less than 15, all of the inclusions were measured. When the number of inclusions exceeded 15, measurements of all different inclusion sizes were taken (from the smallest to the largest). In both cases, the minimum and maximum values of the length of the inclusions of each coprolite are given.
- 4) The arrangements of inclusions in the coprolite matrix are described as fragmented (groups of remains with no anatomic relationship with each other), articulated (some of the remains in anatomical articulation), and isolated (ungrouped and widely separated remains).
- 5) Action of digestive process. As the main feature of digestion processes is the etching of bone surfaces by stomach acids (Fernández-Jalvo and Andrews, 2016), it is possible to record the pitting and corrosion lines on the surfaces of coprolite inclusions; however, the chemical changes caused by digestive enzymes are difficult to observe (Fernández-Jalvo and Andrews, 2016). The following features were studied by SEM analyses: pitting on inclusions and corrosion lines. The variable named 'chemical signals', with three stages, is considered to summarize the combination of pitting and corrosion: light (slight pitting and no/slight corrosion lines); moderate (noticeable pitting and some corrosion lines, or slight pitting and profuse corrosion lines); and heavy (great pitting and marked corrosion lines). In addition,

the shape of fractures at the ends of the inclusions was indicated, if exposed (i.e., blunt, pinched, straight or irregular); when two or more of them were present, this variable was codified as 'all types' (Table 2).

### Morphotypes ordination

The ordering of the morphotypes was explored on the basis of a distance or dissimilarity matrix (Bray-Curtis dissimilarity index, PAST ver. 2.17; Hammer *et al.*, 2001), using the features of undigested food and patterns of the digestive chemical processes per specimen (see Appendix 1). Non-metric, multidimensional scaling (NMDS) is an indirect gradient analysis approach, which produces an ordination and attempts to represent the pairwise dissimilarity between objects in a low-dimensional space. NMDS allows the testing of the relationships between the inclusion properties and the digestive strategies proposed for the morphotypes. The best-fit solution of NMDS was assessed by the stress of the ordination, which measures how reliably the multidimensional relationships among the samples are represented in the two-dimensional ordination plot. Useful two-dimensional plots should have a stress value smaller than 0.2 (Zuschin *et al.*, 2006).

## RESULTS

### Study of properties of inclusions

The study of the properties of the inclusions was carried out on twenty-three specimens that belong to the morphotypes previously indicated. Figures 2 and 3 show examples of coprolites (macroscale photos) and their inclusions (SEM photos). Table 2 includes all the described features explained in the Material and Methods section. These tables comprise the coprolite linear dimensions (length and diameter), a description of the inclusions of the specimen, and the resulting patterns of the digestive chemical processes. See Appendix 2 for a detailed description of the results.

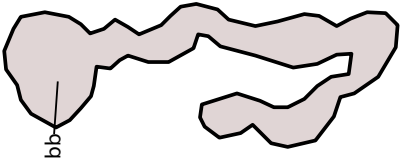
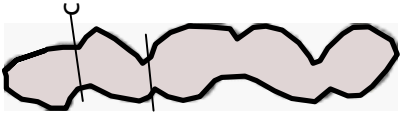
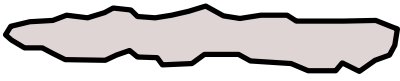
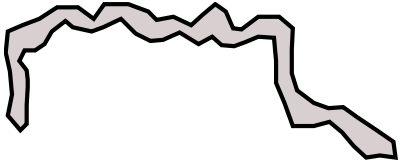
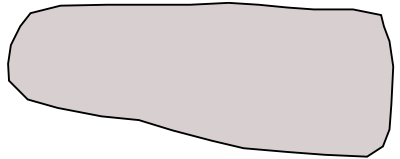
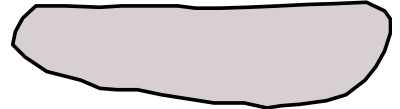
### Size of inclusions by morphotype

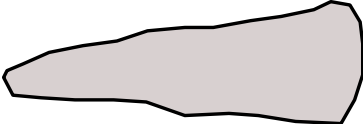
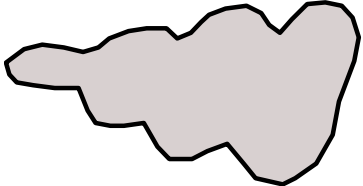
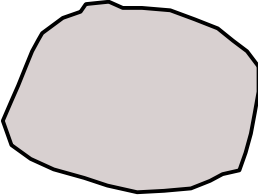
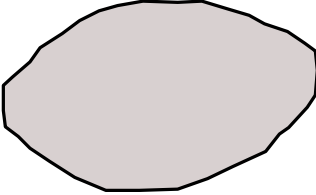
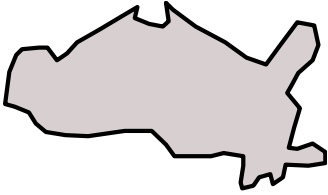
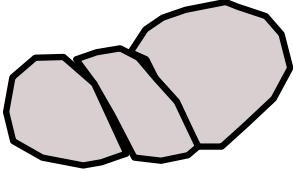
Generally, the average of the size of inclusions for the Las Hoyas coprolites is less than 2 mm (Fig. 4). Circular, bump-headed lace, fir-tree, rosary, straight lace, and thin lace morphotypes show less variation in the size of their inclusions. The median value is asymmetric for cylinder, cone, ellipsoidal and elongated morphotypes, indicating an unequal variation of inclusions size, significant among the large inclusions and minor among the smaller inclusions. The one specimen corresponding to the spiral morphotype is not representative in this sample, because it only shows two exposed inclusions. The irregular morphotype contains a great number of outliers increasing the mean value up to 3 mm in size. An increase in the diameter of the faecal mass is related to longer inclusions (Fig. 5), which is evident in irregular, elongated, and cone specimens and one of the cylinder specimens of more than 7 mm in diameter.

Table 1

The Las Hoyas coprolite association (upper Barremian, Cuenca, Spain). Every morphotype includes a description and a drawing. The lower line corresponds to the classification categories used in Hunt and Lucas (2012), and comprises: Morpho—morphotype; Submo—submorphotype; Producer—coprolite producer.

Abbreviations used for morphotypes are: A—cylindrical, elongated; B—cylindrical, short; C—subrounded; F—spiral; H—thin, ovoid; I—thin, linear; K—irregular shape; NE—no equivalence

| Bump-headed lace   | Rosary  | Straight lace  | Thin lace   | Elongated   | Cylinder  |
|--|---|--|---|---|---|
| <p>One of the ends with a big bulge (bb), at least twice as wide as the rest of the coprolite. The overall shape is elongated cord.</p>  | <p>Series of wide segments with bumps separated by constrictions (c). The overall shape is elongated with bumps.</p>  | <p>Long and straight, unfolded, with a roughly similar diameter throughout the length. The overall shape is elongated cord.</p>  | <p>Folded onto themselves, with a roughly identical diameter throughout their length. The overall shape is ribbon-like.</p>  | <p>The overall shape is rectangular, at least three times longer than wide. Flat ends.</p>  | <p>The overall shape is strongly elongated, with a roughly constant width. Rounded ends.</p>  |
| <p><b>Morpho:</b> NE<br/><b>Submo:</b> NE<br/><b>Producer:</b> NE</p>  | <p><b>Morpho:</b> NE<br/><b>Submo:</b> NE<br/><b>Producer:</b> NE</p>   | <p><b>Morpho:</b> I<br/><b>Submo:</b> Thin Linear<br/><b>Producer:</b> Fish</p>  | <p><b>Morpho:</b> NE<br/><b>Submo:</b> NE<br/><b>Producer:</b> NE</p>   | <p><b>Morpho:?</b> B<br/><b>Submo:</b> ?B4 cylindrical short<br/><b>Producer:</b> NE</p>  | <p><b>Morpho:</b> A<br/><b>Submo:</b> A4 cylindrical elongated<br/><b>Producer:</b> Fish, Anura, Chelonii, Crocodylia, Theropoda</p>  |

|  |   |   |
|--|---|---|
| <p><b>Cone</b></p> <p>Diameter increases throughout the longitudinal axis, no constrictions. Maximum diameter occurs at one end. The overall shape is cone to tear-drop.</p> |  | <p><b>Morpho:</b> B<br/><b>Submo:</b> B2 cylindrical short<br/><b>Producer:</b> ?Fish</p> |
| <p><b>Fir-tree</b></p> <p>Sequence of 'bumps' that decrease progressively from a wide end to a very narrow end. The overall shape is triangular.</p>                         |  | <p><b>Morpho:</b> C<br/><b>Submo:</b> NE<br/><b>Producer:</b> NE</p>                      |
| <p><b>Circular</b></p> <p>Rather flat, but not as flat as a disc. The overall shape is a subrounded and flattened spheroid.</p>  |  | <p><b>Morpho:</b> C<br/><b>Submo:</b> NE<br/><b>Producer:</b> NE</p>                      |
| <p><b>Ellipsoidal</b></p> <p>Diameter wider at the middle, and major axis twice or three times longer than minor axis. The overall shape is roughly ovoid.</p>               |   | <p><b>Morpho:</b> H<br/><b>Submo:</b> Thin-ovoid<br/><b>Producer:</b> Fish</p>            |
| <p><b>Irregular</b></p> <p>Not grouped as defined morphotype. With a varied mosaic of shapes.</p>  |    | <p><b>Morpho:</b> K<br/><b>Submo:</b> Irregular<br/><b>Producer:</b> Fish</p>             |
| <p><b>Spiral</b></p> <p>With spiral marks. Strips with regular widths. The overall shape is elongated.</p>   |    | <p><b>Morpho:</b> F<br/><b>Submo:</b> F2 Amphipolar Spiral<br/><b>Producer:</b> Fish</p>  |

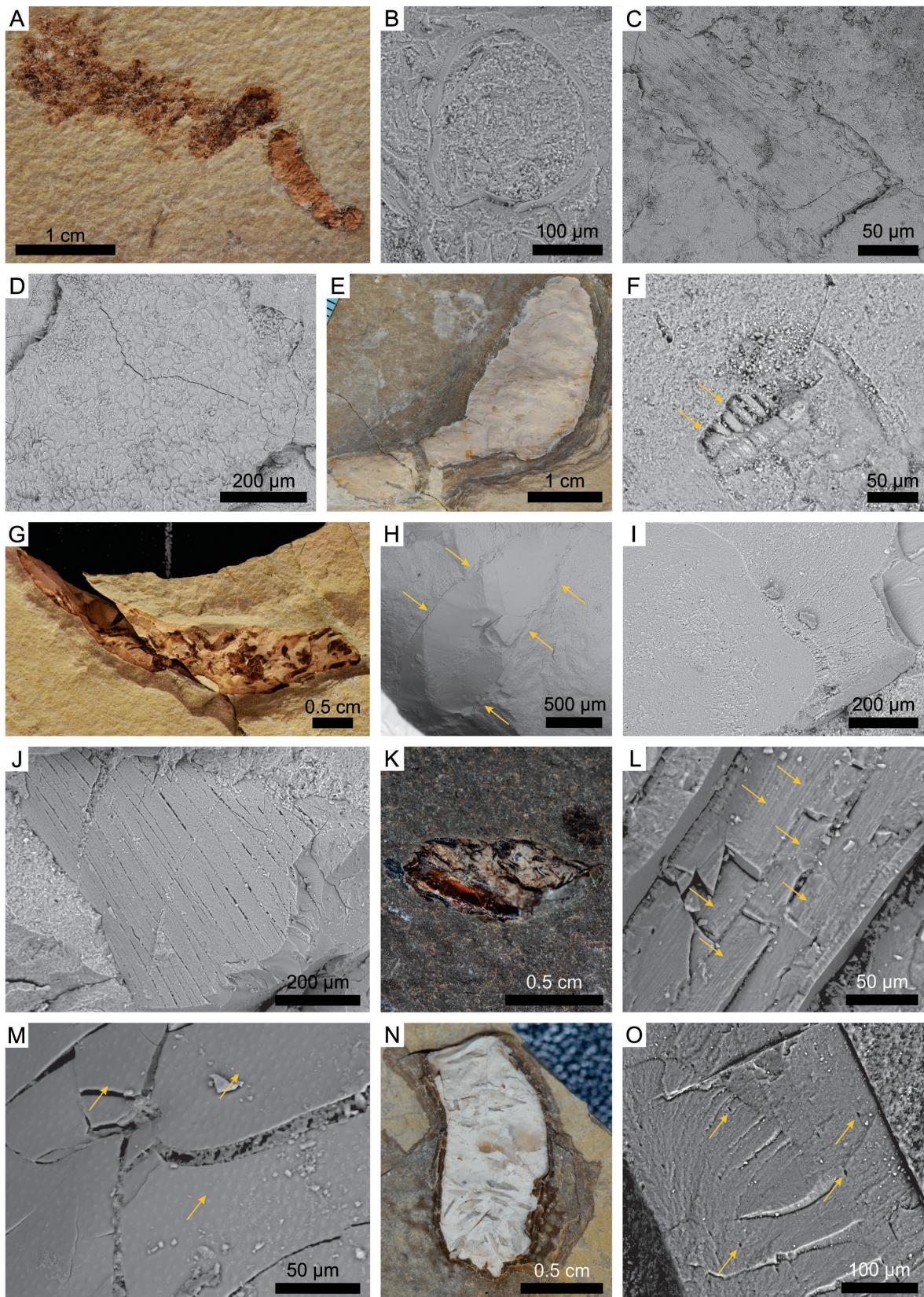


**Fig. 2.** SEM and BSE images of coprolite specimens from the Las Hoyas locality (upper Barremian, Cuenca, Spain). **A.** Bump-headed lace coprolite, MCCM-LH15993a. **B.** MCCM-LH15993a, hollow vertebra. **C.** MCCM-LH15993a, plant remains with parallel fibres. **D.** MCCM-LH15993a, vegetal epidermis. **E.** Cylinder coprolite, MCCM-LH9475A. **F.** MCCM-LH9475A, sequence of teeth or the internal mould of a tiny, grooved, undetermined fragment (? Mollusc, gastropod) indicated by arrow. **G.** Cylinder coprolite, MCCM-LH21486B. **H.** MCCM-LH21486B, shape indicated by arrows. **I.** MCCM-LH21486B, broken bone showing slight pitting. **J.** MCCM-LH21486B, bone with corrosion lines. **K.** Ellipsoidal coprolite, MCCM-LH15929b. **L.** MCCM-LH15929b, lamellated bone structure indicated by arrows. **M.** MCCM-LH15929b, putative bone showing tubercles as ornamentation of a ?ganoid scale, indicated by arrows. **N.** Elongated coprolite, MCCM-LH-LI15-001B. **O.** MCCM-LH-LI15-001B, bone showing noticeable pitting, indicated by arrows.

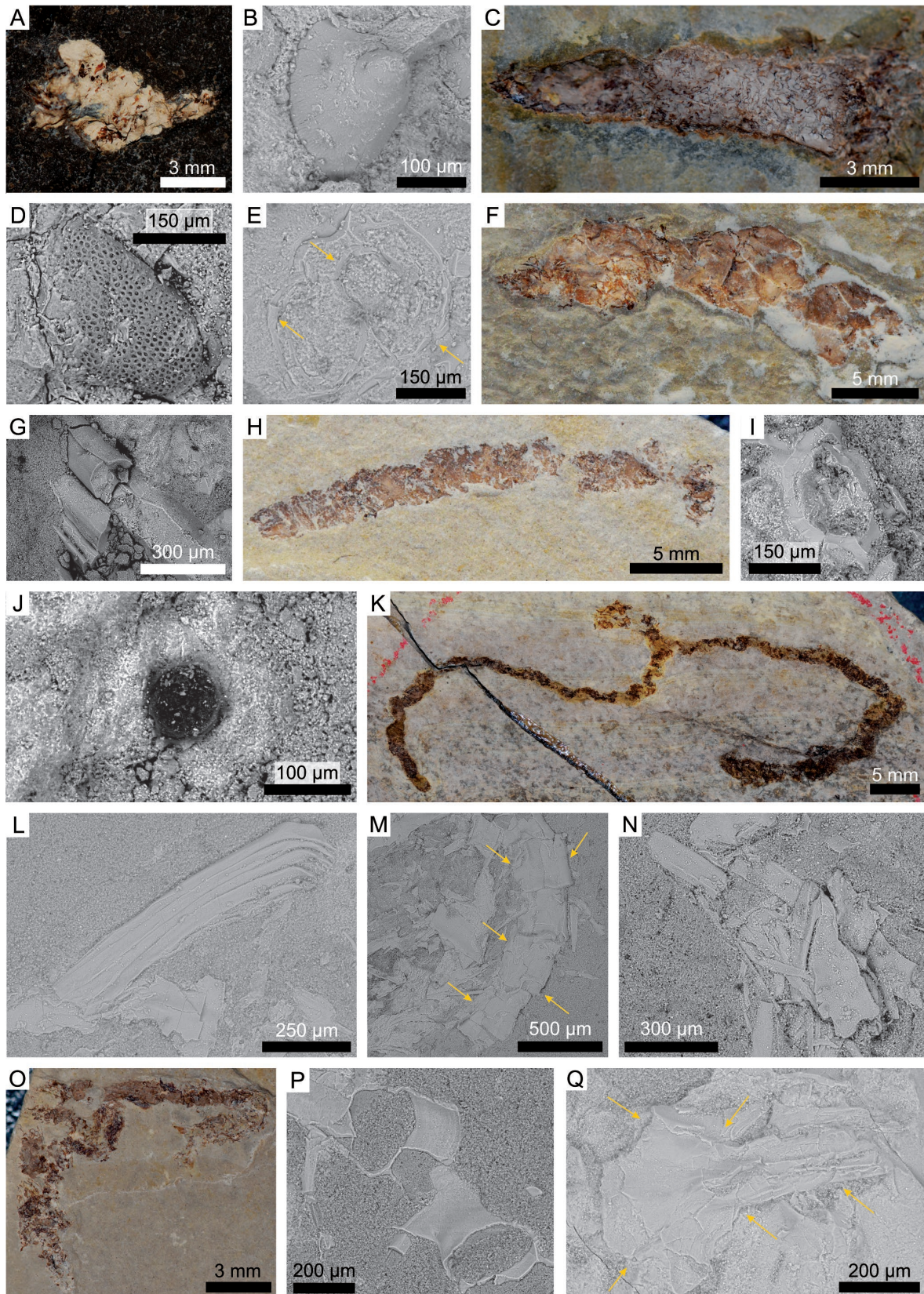


**Fig. 3.** SEM and BSE images of coprolite specimens from the Las Hoyas locality (upper Barremian, Cuenca, Spain). **A.** Fir-tree coprolite, MCCM-LH32378 **B.** Putative tooth, MCCM-LH32378. **C.** Irregular coprolite, MCCM-LH28253a. **D.** Ostracod valve, MCCM-LH28253a. **E.** Broken putative vertebrae indicated by arrows, MCCM-LH28253a. **F.** Rosary coprolite, MCCM-LH23541A. **G.** Putative broken ribs, MCCM-LH23541A. **H.** Straight lace coprolite, MCCM-LH20198b. **I.** Big vertebra with lamellar bone, MCCM-LH20198b. **J.** Coalified plant structure, MCCM-LH20198b. **K.** Thin lace coprolite, MCCM-LH-GQ17-030a. **L.** Striated bone, MCCM-LH-GQ17-030a. **M.** Articulated vertebrae indicated by arrows, MCCM-LH-GQ17-030a. **N.** Overlapping bones, MCCM-LH-GQ17-030a. **O.** Thin lace coprolite, MCCM-LH-LI15-028B. **P.** Vertebrae with broken ribs anchored, MCCM-LH-LI15-028B. **Q.** Probable fish palate indicated by arrows, MCCM-LH-LI15-028B.

Table 2

Characterization of the Las Hoyas coprolite association: size, inclusion features, and patterns of the digestive chemical processes.  
 Abbreviations: NI – number of inclusions; IS – inclusion size; ID – inclusion identification; IA – inclusion arrangement;  
 PC – pitting and corrosion; FE – shape of the fractures observed at the ends; CS – chemical signal.

| Morphotype Specimen number                              | Coprolite size (mm)                                   | NI    | IS (mm)                              | ID  | IA                           | PC                                 | FE                        | CS  |
|---|---|-------|--------------------------------------|---|------------------------------|------------------------------------|---------------------------|---|
| Bump-headed lace<br><b>MCCM-LH15993a</b><br>(Fig. 2A–D) | Length: 39.6<br>Diameter: 3.3<br>mid part; 9<br>bulge | >45   | 0.2–0.9                              | Nature: Vertebrate (fish). Elements:<br>plant parts: Section of a hollow<br>vertebra and parallel fibres, vegetal<br>epidermis  | Fragmented and<br>overlapped | Pitting<br>No corrosion lines      | All types                 | Light   |
| Bump-headed lace<br><b>MCCM-LH35393</b>                 | Length: 40<br>Diameter: 3 mid<br>part; 9 bulge        | >45   | 0.4–0.8<br>In the bulge: 1.3–1.6     | Nature: Vertebrate (fish): branchial<br>arch, ribs  | Fragmented and<br>overlapped | Pitting<br>Some corrosion<br>lines | Irregular and<br>straight | Light   |
| Circular<br><b>MCCM-LH21425b</b>                        | Diameter<br>ca. 4.4                                   | <15   | 0.2–0.9<br>Largest inclusion:<br>1.6 | Nature: Bony fragments  | Isolated                     | Pitting<br>No corrosion lines      | All types                 | Light   |
| Circular<br><b>MCCM-LH26943b</b>                        | Diameter<br>ca. 5.5                                   | 31–45 | 0.3–1.1                              | Nature: Vertebrate (fish): Fish scales  | Isolated                     | Pitting<br>Some corrosion<br>lines | All types                 | Light   |
| Cylinder<br><b>MCCM-LH9475A</b><br>(Fig. 2E–F)          | Length: 49<br>Diameter: 14.5                          | <15   | Not at macroscale                    | Nature: Vertebrate (?fish); arthropod,<br>mollusc (gastropod)<br>part= isolated: sequence of ?teeth<br>indeterminate or the internal mould of<br>a tiny ?mollusc/?arthropod | Not applicable               | Not applicable                     | Not applicable            | Not applicable  |
| Cylinder<br><b>MCCM-LH21486B</b><br>(Fig. 2G–J)         | Length: 50.3<br>Diameter: 9                           | 31–45 | 1.2–4.6<br>Largest inclusion:<br>5.7 | Nature: Vertebrate (fish): Fish scales  | Isolated                     | Pitting<br>Corrosion lines         | All types                 | Moderate<br>(pitting more<br>extensive than<br>corrosion) |
| Cylinder<br><b>MCCM-LH28719a</b>                        | Length: 41.2<br>Diameter: 11                          | <15   | Not at macroscale                    | Nature: Small and isolated bony<br>inclusion  | Not applicable               | Not applicable                     | Not applicable            | Not applicable  |
| Cylinder<br><b>MCCM-LH-LH15-019</b>                     | Length: 14<br>Diameter: 3.8                           | >45   | 0.2–1.1                              | Nature: Vertebrate (fish): Possible fish<br>ribs and a fish scale in section cut  | Isolated                     | Pitting<br>No corrosion lines      | All types                 | Light   |
| Cone<br><b>MCCM-LH16609B</b>                            | Length: 15.5<br>Diameter: 9                           | 15–30 | 0.2–2.2                              | Nature: Vertebrate (fish): Scales and<br>bony remains   | Isolated                     | Pitting<br>Corrosion lines         | Blunt and<br>straight     | Moderate<br>(corrosion<br>greater than<br>pitting)        |

| Morphotype Specimen number                            | Coprolite size (mm)           | NI    | IS (mm)                              | ID   | IA                      | PC                                     | FE                | CS  |
|---|-------------------------------|-------|--------------------------------------|--|-------------------------|--|-------------------|---|
| Ellipsoidal<br><b>MCCM-LH15929b</b><br>(Fig. 2K-M)    | Length: 10<br>Diameter: 4     | 30-45 | 0.5-1.7<br>Largest inclusion:<br>6.8 | Nature: Vertebrate (fish): ?ganoid scale, others with lamellated bone structure  | Isolated and fragmented | Pitting<br>Some corrosion lines        | All types         | Light                                     |
| Elongated<br><b>MCCM-LH-LH115-001B</b><br>(Fig. 2N-O) | Length: 14.2<br>Diameter: 6.6 | 15-30 | 0.7-2.9                              | Nature: Bony fragments   | Isolated                | Pitting<br>Corrosion lines             | Blunt and pinched | Moderate (pitting greater than corrosion) |
| Elongated<br><b>MCCM-LH-LH115-002A</b>                | Length: 13.2<br>Diameter: 8.3 | 15-30 | 0.3-4.3                              | Nature: Bony fragments   | Isolated                | Pitting<br>Corrosion lines             | Blunt             | Moderate (pitting greater than corrosion) |
| Fir-tree<br><b>MCCM-LH32378B</b><br>(Fig. 3A-B)       | Length: 9<br>Diameter: 4.2    | >45   | 0.2-1                                | Nature: Vertebrate: Small tooth and bony fragments   | Isolated and fragmented | Pitting<br>Some corrosion lines        | All types         | Light                                     |
| Irregular<br><b>MCCM-LH20124</b>                      | Length: 40<br>Diameter: 26.5  | <15   | Not at macroscale                    | Nature: Small isolated tubular inclusion   | Not applicable          | Not applicable                         | Not applicable    | Not applicable                            |
| Irregular<br><b>MCCM-LH27015A</b>                     | Length: 30<br>Diameter: 12.5  | 15-30 | 0.5-13                               | Nature: Bony fragments   | Isolated and fragmented | Great pitting<br>Corrosion lines       | Blunt             | Heavy                                     |
| Irregular<br><b>MCCM-LH28253A</b><br>(Fig. 3C-E)      | Length: 15.5<br>Diameter: 4.2 | >45   | 0.2-0.6                              | Nature: Vertebrate (fish); Elements: Crustacean (ostracod, ? <i>Cypridea</i> ): vertebrae and ribs; valve  | Fragmented              | Slight pitting<br>No corrosion lines   | All types         | Light                                     |
| Rosary<br><b>MCCM-LH23541A</b><br>(Fig. 3F-G)         | Length: 23<br>Diameter: 5.3   | >45   | 0.4-2.2                              | Nature: Vertebrate (?fish): Broken ribs  | Fragmented              | No pitting<br>Some corrosion lines     | Irregular         | Light                                     |
| Spiral<br><b>MCCM-LH22349</b>                         | Length: 10.4<br>Diameter: 4.8 | <15   | 0.3-0.5                              | Nature: Two small inclusions   | Isolated                | Not applicable                         | Not applicable    | Not applicable                            |
| Straight lace<br><b>MCCM-LH16611A</b>                 | Length: 11.5<br>Diameter: 2   | >45   | 0.2-0.8                              | Nature: Vertebrate part: broken ?vertebra  | Fragmented              | Slight pitting<br>Some corrosion lines | All types         | Light                                     |
| Straight lace<br><b>MCCM-LH20198B</b><br>(Fig. 3H-J)  | Length: 28<br>Diameter: 2.8   | >45   | 0.2-0.8                              | Nature: Vertebrate (fish); Elements: plant parts: fish vertebra with lamellar bone, coalified plant structure, tubular bony structures (probably ribs) | Fragmented              | Slight pitting<br>No corrosion lines   | All types         | Light                                     |
| Thin lace<br><b>MCCM-LH16564A</b>                     | Length: 19.5<br>Diameter: 2   | >45   | 0.3-1.2                              | Nature: Bony fragments   | Fragmented              | Slight pitting<br>No corrosion lines   | All types         | Light                                     |

Table 2

Continuation from the former pages.

| Morphotype<br>Specimen number                      | Coprolite size<br>(mm)       | NI  | IS (mm) | ID   | IA                                     | PC                                 | FE        | CS    |
|--|------------------------------|-----|---------|--|--|------------------------------------|-----------|-------|
| Thin lace<br>MCCM-LH-GQ-<br>17-030A<br>(Fig. 3K-N) | Length: 100<br>Diameter: 2.2 | >45 | 0.3–1.3 | Nature: Vertebrate (fish): Several groups of articulated vertebrae, fish rays and ribs   | Fragmented, overlapped and articulated | Pitting<br>Some corrosion lines    | All types | Light |
| Thin lace<br>MCCM-LH-LJ15-<br>028B<br>(Fig. 3O-Q)  | Length: 25<br>Diameter: 2.5  | >45 | 0.2–0.7 | Nature: Vertebrate (fish): Vertebrae (some partially articulated with anchored ribs), radius from fins and a palate from macrosemiid fish ( <i>Notogogus</i> ) or a juvenile teleost | Fragmented                             | No pitting<br>Some corrosion lines | All types | Light |

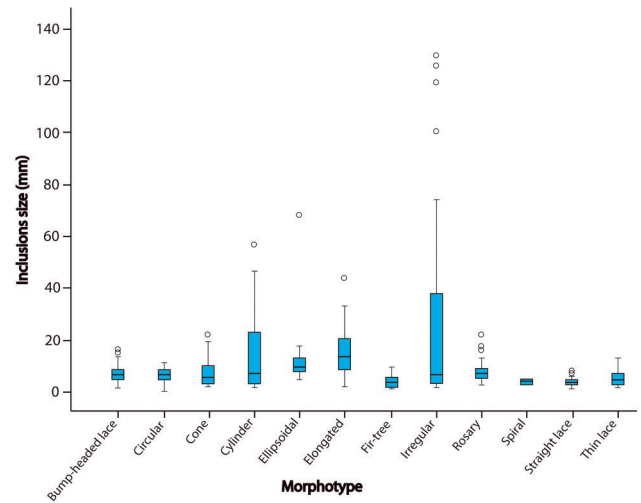


**Fig. 4.** Box-plot graphic representing size values of inclusions for the different morphotypes. Circles represent the outliers for the corresponding morphotype, the box represents the percentiles, the thin line represents the median, and whiskers represent the minimal and maximal values.

#### Non-Metric Multidimensional Scaling (NMDS) analysis

The NMDS analysis clearly separates the morphotypes into at least three groups. The NMDS has a stress value of 0.085 and is therefore reliable for describing the relationships among the samples in two-dimensional ordination plots (Clarke and Warwick, 2001; Zuschin *et al.*, 2006). In Figure 6, the dots that are close together represent morphotypes that are very similar, regarding the taphonomic properties of the inclusions; the dots that are far apart have different values and even in the sample some have missing values (i.e., 18SPI, 7 and 5 CYL and 14 IRR in Fig. 6). The NMDS shows the interplay between the number of inclusions and their arrangement in the coprolite matrix along the y-axis, and the intensity of chemical signals along the x-axis of the graph. The group of positive y values and negative x values defines coprolites that are densely filled and have fragmented to overlapped inclusions, with light chemical signals (bump-headed lace (BHL); fir-tree (FIR); rosary (RO); straight lace (STR); and thin lace (TH) morphotypes). The second group (circular (CIR); spiral (SPI); and cylinder (CYL) morphotypes) are scarcely filled, with isolated inclusions, and slight chemical signals. The third group, comprising the cone (CO); and elongated (ELO) morphotypes, occupies the positive x values, because its members share a moderate degree of corrosion and pitting.

A minimum spanning tree was also constructed to show the total minimal distance connecting all points, to visualize the grouping close points. All the same morphotypes, except for irregular (IRR), are placed within the same group. Closer points are in the upper left of the plot, corresponding also to coprolites with lower diameters (Fig. 5); note that the coprolite diameter increases towards the positive values of the x-axis (see Figs 5, 6).

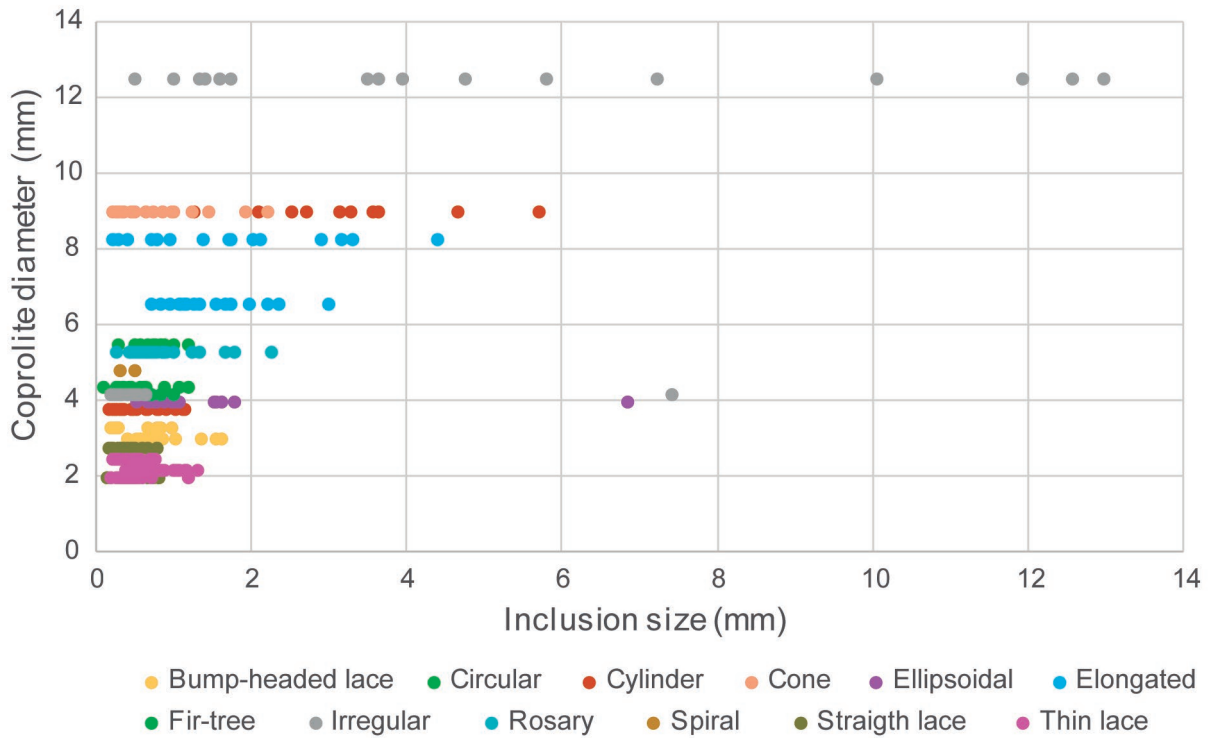


**Fig. 5.** Graphic showing the relationship between size values of inclusions and coprolite maximum diameter. The data are given representing every morphotype by means of different colours. For bump-headed lace coprolites, the diameter represented is the diameter of the coprolite cord.

### DISCUSSION

The present study was designed to establish the type of correlation that exists between the coprolite morphotypes and the alterations in the coprolite inclusions, due to the digestive strategies of the producers. In order to arrange a representative sample (e.g., Rodríguez-de la Rosa *et al.*, 1998; Luo *et al.*, 2017; Dentzien-Diaz *et al.*, 2018) and to test the similarity of the observed taphonomic properties of the inclusions, more than one specimen for each morphotype was included (except for cone, ellipsoidal, fir-tree, rosette and spiral morphotypes) and around 500 inclusions were counted and observed, combining lower magnifications and SEM, to provide a more relevant taphonomic description (Butler and Schroeder, 1998).

The features observed in the specimens show enough shared similarities to make some generalizations about the morphotypes and discuss how these are ordered. This is particularly relevant for the circular, cylinder, bump-headed lace, elongated, straight lace and thin lace morphotypes. In the irregular morphotype, the variation of the taphonomic features and the type of inclusions were not consistent among specimens. This variation indicates that the morphotype could have been a compilation of non-definable shapes, ingestions and/or producers. In these cases and in the ones represented by only one specimen (cone, ellipsoidal, fir-tree, rosette and spiral), new specimens should be analysed to confirm the degree of consistency of digestive alteration among specimens per morphotype.

The sizes of the Las Hoyas coprolites and the fact that they mostly contain bone fragments suggest that most were

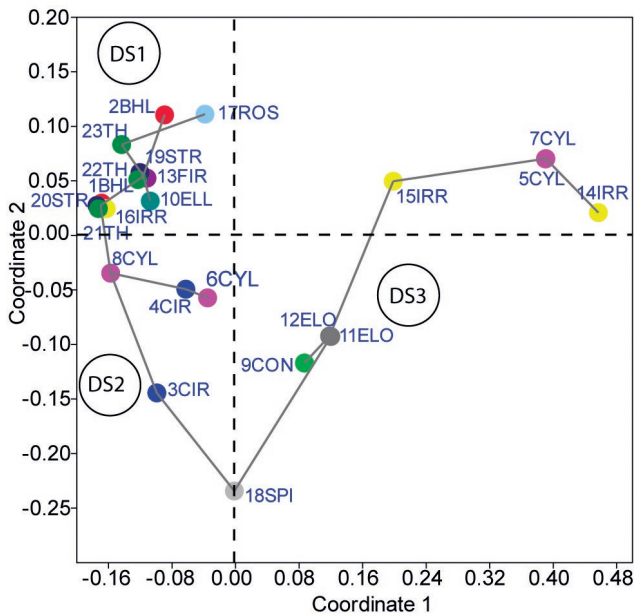


**Fig. 6.** Non-metric Multidimensional Scaling (NMDS) ordination. The graph represents the relationships among samples according to the taphonomic properties analyzed for the coprolite inclusions. The line connecting the dots is the Minimum Spanning Tree. DS1 = digestive strategy 1; DS2 = digestive strategy 2; DS3 = digestive strategy 3.

produced by vertebrate predators (Barrios-de Pedro *et al.*, 2018a, b). All the selected taphonomic properties were combined to assess the ways of ingestion and the digestive processes, and to furnish the different digestive strategies found from the coprolite association.

### Way of ingestion

The term ‘way of ingestion’ refers to the mechanism used to ingest the prey (e.g., swallowing, chewing, crushing, tearing apart, chopping, cutting; e.g., Diefenbach, 1975; Steven and Hume, 1995; Gutiérrez, 1998; Fernández-Jalvo and Andrews, 2016). The producers of the coprolite morphotypes, showing a higher number of inclusions (> 45) and with partially fragmented and occasionally overlapped remains, could have ingested their food with limited mechanical processing of the food in the mouth. In the thin lace morphotype, some of the inclusions even appear to be articulated in successive packages (Fig. 7), indicating that the prey would have been swallowed whole. In contrast, the producers of coprolites with relatively low numbers of inclusions (< 45) and with mostly unidentifiable remains probably would have masticated (chewed, torn apart, chopped or cut) their prey. The way of ingestion seems to be relevant because food breakage increases the effects of the digestion process, allowing digestive juices to penetrate into cavities, and then increasing the bone area exposed to gastric acids (He and Wurtsbaugh, 1993; Fernández-Jalvo and Andrews, 2016).

### Digestive process

The term ‘digestive process’ refers to the chemical signals left during digestion. The levels of acidity in the predators’ stomachs and the type of digestive enzymes are two factors controlling digestion. The former is the main modifying agent of the surfaces of inclusions and requires time to operate, while the latter breaks down the organic constituents of bones, modifying their internal structure (e.g., Diefenbach, 1975; Butler and Schroeder, 1998; Pinto-Lona and Andrews, 1999; Fernández-Jalvo and Andrews, 2016). In general, the inclusions are more easily identified in morphotypes that show a minor degree of chemical signals (bump-headed lace, ellipsoidal, fir-tree, rosary, straight lace and thin lace), while in those exhibiting a moderate degree of chemical signals the identification of inclusions is difficult or almost impossible. The most identifiable elements are scales and vertebrae, but it was impossible to provide a list of bony elements by skeletal part (see Butler and Schroeder, 1998), even for the cases with a higher abundance of inclusions, because they are fragmented, deformed, and compressed.

The modifications due to digestion (e.g., the shape of the edges of the inclusions, and the splitting and thinness of the bone surface) are the most valuable evidence of diet (Andrews and Fernández-Jalvo, 1998; Pinto-Lona and Andrews, 1999). The features have been mostly applied in the study of archaeological sites (e.g., Pinto-Lona and Andrews, 1999; Tappén and Wrangham, 2000). The present authors

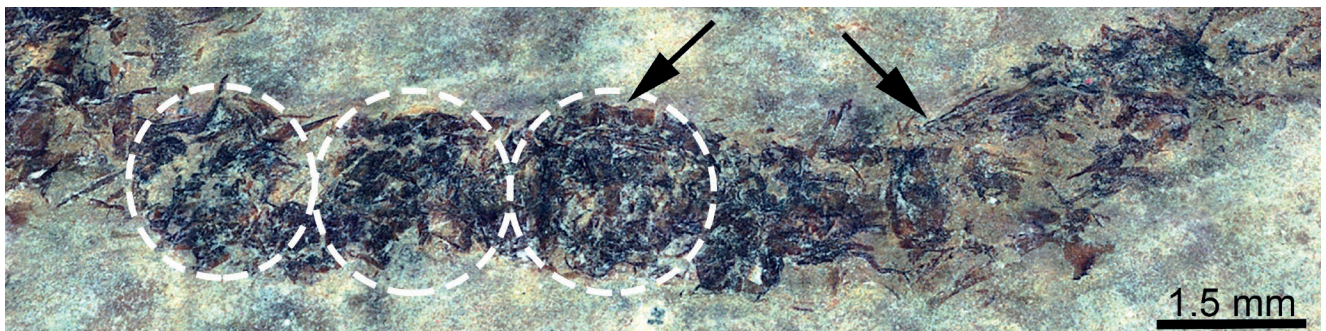


**Fig. 7.** Detail of the central part of the thin lace coprolite MCCM-GQ17-030A, showing packages of inclusions (dashed lines) with articulated elements (indicated by arrows). Image taken with a 3D high-resolution microscope with interferometric and profilometry in a focus variation mode.

The morphotypes rich in undigested food remains (bump-headed lace, fir-tree, rosary, straight lace, and thin lace) display a similar size range of inclusions and the mean value of the inclusions is the smallest (around 1 mm; Fig. 4). This, together with the observation that the inclusions identified correspond mostly to small fishes, indicates that the producers probably fed on the same sort of prey. In the scarcely filled morphotypes (cylinder, cone, ellipsoidal, and elongated), the range of the size of inclusions is heterogeneous and the larger inclusions even reach more than 4 mm in length. The producers of such morphotypes probably would have fed on a different kind of prey, most likely slightly larger animals than those in the first group of morphotypes (Fig. 5), which would indicate a relationship between the size of the prey and the coprolite producer.

have evaluated some of these features, but they are obviously more difficult to discern since the inclusions are partially covered and some even overlap. Nonetheless, in general, the Las Hoyas coprolite association is characterized by bearing a minor degree of corrosion and pitting, and most of the fractures at the ends of inclusions are varied and even include morphotypes with sharp or rectilinear edges (Fig. 3L). The strongest action of acids, resulting in round and smooth edges of inclusions, the splitting of bone surfaces with longitudinal lines following the bone weakness, and the thinning of bone walls, were observed in the irregular, cone and elongated morphotypes. Thinness leads to inward curving and the collapsing of the thinned edges of bones (Pinto-Lona and Andrews, 1999), a condition observed, for instance, in specimen MCCM-LH28253a (Fig. 3E).

### Digestive strategies

NMDS analysis (Fig. 6) provided the basis for outlining the different digestive strategies of the Las Hoyas ecosystem with regard to the coprolite association. The digestive strategies can be distinguished by linking food intake and digestion process. The first one (Fig. 6, DS1) includes a diverse number of morphotypes and owing to the completeness and abundance of inclusions the strategy would correspond to animals with low digestive assimilation. It is characterized by a food intake of one or several prey with limited processing in the mouth. The food eaten would be accumulated in the digestive system for a short time and/or the digestive process would exhibit low acid content (Owocki *et al.*, 2012; Luo Mao *et al.*, 2017). This strategy would only make sense in a scenario, where food was very abundant and nourishment was guaranteed (Cork and Kenagy, 1989). Of particular interest is the thin lace coprolite MCCM-LH-GQ17-030A (22TH in Fig. 6), because the producer ingested more than one prey in a short period of time, which indicates the special voracity of the predator, compared with other producers of the same coprolite morphotype.

The second digestive strategy (Fig. 6, DS2) contains a limited number of morphotypes, and owing to the reduction and breakage of undigested food, the strategy indicates an improved digestive assimilation. It is characterized by mastication prior to deglutition that might be enhanced by gastric motility in the stomach (Diefenbach, 1975; Davenport *et al.*, 1990). It also would be associated with a longer retention time and food processing by the digestive system of the producer, which could indicate a more effective and/or longer digestion (Steven and Hume, 1995; Luo Mao *et al.*, 2017). A longer digestion would be enhanced by increasing the volume and the length of the digestive system of the predators. This fact would favour the retention time of food in the organism and therefore increase the digestion rate and the absorption of nutrients in the intestine (Bozinovic, 1993).

A possible third digestive strategy (Fig. 6, DS3) has a limited number of morphotypes, and the fragmented inclusions with abundant chemical signals indicate an efficient digestive strategy. It combines scarcity of food remains, large inclusions in coprolites with wider diameters, and important chemical signals of pitting and corrosion and even the blunting of edges. This combination indicates that the mechanism used to ingest the prey could have also included mastication (e.g., crushing and tearing apart), but above all a more efficient chemical digestion with food retained for a long time in the digestive system.

### Feeding groups

The feeding ecology of the Las Hoyas Barremian ecosystem, on the basis of the coprolite association, can be characterized as: 1) a lentic environment enriched in prey, owing to the abundance of inclusions, as is reflected in the body fossil record; 2) having a greater diversity in morphotypes with a swallowing or non-processed ingestion; 3) having a limited diversity of morphotypes, greater in diameter, with varied

mastication ingestion and rather more efficient digestion. The swallower group contains a variety of thin-narrow and long coprolites that could have been produced by species of animals able to swallow whole prey such as fishes, frogs, birds, and lizards. The other group would include larger predators able to capture and process larger prey. From all the potential producers, it is clear that crocodiles could have formed part of this group. They ingest food in large pieces, with minor mechanical breakdown in the mouth; the reduction in size of the food and its chemical degradation occurs mainly in the stomach, enhanced by the motility of this organ and by gastroliths; and they retain the food in the digestive system for a long period of time (Diefenbach, 1975; Davenport *et al.*, 1990). Morphotypes included in the third strategy (elongated to conical) match the shape of extant crocodylian faeces (Milán, 2012).

### CONCLUSIONS

The study of inclusions in coprolites provides information not only about the prey that the producers ingested, but also about the digestive processes of the predators. The study of digestive alterations previously was applied mainly in coprolites found at archaeological sites. In this study, the authors have applied non-destructive techniques to identify, quantify, and estimate the degree of alteration of coprolite inclusions, which reflects the intake and the digestive secretions of the coprolite producers. This has allowed characterization of the whole Las Hoyas coprolite association, the producers of which were predominately vertebrate predators. Although the authors have found some ostracod and plant remains, they have not been able to verify the presence of insects or crustaceans in the coprolites. Given the great diversity of coprolite morphotypes found in this lacustrine environment, this study has allowed the establishment of correspondence between morphotypes and the types of alteration of the inclusions due to digestion. The results show that there is no unambiguous correspondence between morphotypes and inclusion properties, as there are several morphotypes that share the same type of digestive features in their inclusions. The features used have been useful in ordering and characterizing different types of digestive strategies. Accordingly, the authors propose up to three types of digestive strategy for the coprolite producers: the first involves a limited processing in the mouth, a short retention time of food, and/or a low efficiency of the digestive system; the second implies possible mastication of food prior to deglutition, followed by a longer retention time of food in the digestive system; and the third includes a group with mastication, long retention time of food, and more effective digestion. This contribution is a first step in the understanding of the feeding ecology of this Barremian wetland ecosystem, based on the coprolite association.

### Acknowledgements

The authors thank Santiago Langreo and Mercedes Llandres at the Museo de las Ciencias de Castilla-La Mancha for allowing access to the coprolite collection. Special thanks go to Alberto Jorge and Marta Furio at the Museo Nacional de Ciencias Naturales for

carrying out the SEM analyses; as well as to Cristina Paradela for carrying out the 3D surface measurement with the 3D high-resolution microscope. Thanks also go to Miguel Angel Fernandez of the Department of Biology at the Universidad Autónoma de Madrid for the digital camera. Comments and correction of the original manuscript by Spencer G. Lucas (New Mexico Museum of Natural History and Sciences) and Martin Qvarnström (Uppsala University, Sweden) improved the study. Funds were provided by the MINECO reference CGL2013-42643-P. The fellowship reference BES-2014-070985 of the Program for the Training of Researchers of the MINECO is associated with this project.

## REFERENCES

- Andrews, P. & Fernandez-Jalvo, Y., 1998. 101 uses for fossilized faeces. *News and Views of Nature*, 393: 629–630.
- Bailleul, A., Ségalen, L., Buscalioni, A. D., Cambra-Moo, O. & Cubo, J., 2011. Palaeohistology and preservation of tetrapods from Las Hoyas (Lower Cretaceous, Spain). *Comptes Rendus Palevol*, 10: 367–380.
- Barrios-de Pedro, S., Poyato-Ariza, F. J., Moratalla, J. J. & Buscalioni, A. D., 2018a. Exceptional coprolite association from the Early Cretaceous continental Lagerstätte of Las Hoyas, Cuenca, Spain. *PLoS ONE* 13 (5): e0196982.
- Barrios-de Pedro, S., Poyato-Ariza, F. J., Moratalla, J. J. & Buscalioni, A. D., 2018b. An exceptional coprolite assemblage from Las Hoyas fossil site (La Huérguina Formation, Cuenca, Spain). In: Bordy, E. M. (ed.), *Proceedings of the 2nd International Conference of Continental Ichnology (ICCI 2017), Nuy Valley (Western Cape Winelands), 1–8 October 2017. Palaeontologia Africana*, 52: 141–142.
- Bozinovic, F., 1993. Fisiología ecológica de la alimentación y digestión en vertebrados: modelos y teorías. *Revista Chilena de Historia Natural*, 66: 375–382.
- Buatois, L. A., Mángano, M. G., Fregenal-Martínez, M. A. & Gibert, J. M., de, 2000. Short-term colonization trace-fossil assemblages in a carbonate lacustrine Konservat-Lagerstätte (Las Hoyas fossil site, Lower Cretaceous, Cuenca, Central Spain). *Facies*, 43: 145–156.
- Buscalioni, A. D. & Fregenal-Martínez, M. A., 2010. A holistic approach to the palaeoecology of Las Hoyas Konservat-Lagerstätte. In: Buscalioni, A. D. & Fregenal-Martínez, M. A. (eds), *Mesozoic Terrestrial Ecosystems and Biotas. Journal of Iberian Geology, Special Volume*, 36: 297–326.
- Buscalioni, A. D. & Poyato-Ariza, F. J., 2016. Las Hoyas: a unique Cretaceous ecosystem. In: Khosla, A. & Lucas, S. G. (eds), *Cretaceous Period: Biotic Diversity and Biogeography. New Mexico Museum of Natural History and Science, Bulletin*, 71: 51–63.
- Butler, V. L. & Schroeder, R. A., 1998. Do digestive processes leave diagnostic traces on fish bones? *Journal of Archaeological Science*, 25: 957–971.
- Clarke, K. R. & Warwick, R. M., 2001. *Change in Marine Communities: An Approach to Statistical Analysis and Interpretation, 2nd Edition*. PRIMER-E, Plymouth, 176 pp.
- Cork, S. J. & Kenagy, G. J., 1989. Nutritional values of hypogeous fungus for a forest-dwelling ground squirrel. *Ecology*, 70: 577–586.
- Davenport, J., Grove, D. J., Cannon, J., Ellis, T. R. & Stables, R., 1990. Food capture, appetite, digestion rate and efficiency in hatchling and juvenile *Crocodylus porosus*. *Journal of Zoology*, 200: 569–592.
- Diefenbach, C. O. C., 1975. Gastric function in *Caiman Crocodylus* (Crocodylia: Reptilia)-I. Rate of gastric digestion and gastric motility as a function of temperature. *Comparative Biochemistry and Physiology*, 51(A): 259–265.
- Dentzien-Diaz, P., Carrillo-Briceño, J. D., Francischini, H. & Sánchez, R., 2018. Paleocological and taphonomical aspects of the Late Miocene vertebrate coprolites (Urumaco Formation) of Venezuela. *Palaeogeography, Palaeoclimatology, Palaeoecology*, 490: 590–603.
- Eriksson, M. E., Lindgren, J., Chin, K. & Mansby, U., 2011. Coprolite morphotypes from the Upper Cretaceous of Sweden: novel views on an ancient ecosystem and implications for coprolite taphonomy. *Lethaia*, 44: 455–468.
- Fernández-Jalvo, Y. & Andrews, P., 2016. *Atlas of Taphonomic Identifications: 1001+ Images of Fossil and Recent Mammal Bone Modification. Vertebrate Paleobiology and Paleoanthropology*. Springer Science+Business Media, Dordrecht, 359 pp.
- Fregenal-Martínez, M. & Meléndez, N., 2016. Environmental reconstruction: a historical review. In: Poyato-Ariza, F. J. & Buscalioni, A. D. (eds), *Las Hoyas: A Cretaceous Wetland*. Dr. Friedrich Pfeil Verlag, München, pp. 14–28.
- Fregenal-Martínez, M. A., Meléndez, N., Muñoz-García, M. B., Elez, J. & Horra, R., de la, 2017. The stratigraphic record of the Late Jurassic-Early Cretaceous rifting in the Alto Tajo-Serranía de Cuenca region (Iberian Ranges, Spain): genetic and structural evidences for a revision and a new lithostratigraphic proposal. *Revista de la Sociedad Geológica de España*, 30: 113–142.
- Furness, J. B., Cottrell, J. J. & Bravo, D. M., 2015. Comparative gut physiology symposium: comparative physiology of digestion. *American Society of Animal Science*, 93: 485–491.
- Gibert, J. M., de, Moratalla, J. J., Mángano, M. A. & Buatois, L. A., 2016. Ichnoassemblage (trace fossils). In: Poyato-Ariza, F. J. & Buscalioni, A. D. (eds), *Las Hoyas: A Cretaceous Wetland*. Dr. Friedrich Pfeil Verlag, München, pp. 195–201.
- Guerrero, M. C., López-Archilla, A. I. & Iniesto, M., 2016. Microbial mats and preservation. In: Poyato-Ariza, F. J. & Buscalioni, A. D. (eds), *Las Hoyas: A Cretaceous Wetland*. Dr. Friedrich Pfeil Verlag, München, pp. 220–228.
- Gutiérrez, G., 1998. Estrategias de forrajeo. In: Ardila, R., López, W., Pérez, A. M., Quiñones, R. & Reyes, F. (eds), *Manual de Análisis experimental del comportamiento*. Librería Nueva, Madrid, pp. 359–381.
- Hammer, O., Harper, D. A. T. & Ryan, P. D., 2001. PAST: Paleontological Statistics software package for education and analysis. *Palaeontologia Electronica*, 4(1): 9 pp.
- He, H. & Wurtsbaugh, W. A., 1993. An empirical model of gastric evacuation rates of fish and an analysis of digestion in piscivorous brown trout. *Transactions of the American Fisheries Society*, 122: 717–730.
- Hunt, A. P. & Lucas, S. G., 2012. Descriptive terminology of coprolites and recent feces. In: Hunt, A. P., Milán, J., Lucas, S. G. & Spielmann, J. A. (eds), *Vertebrate Coprolites. New Mexico Museum of Natural History & Science, Bulletin*, 57: 153–160.
- Hunt, A. P., Lucas, S. G., Milán, J. & Spielmann, J. A., 2012. Vertebrate coprolite studies: Status and prospectus. In: Hunt, A. P.,

- Milán, J., Lucas, S. G. & Spielmann, J. A. (eds), *Vertebrate Coprolites. New Mexico Museum of Natural History & Science, Bulletin*, 57: 5–24
- Iniesto, M., López-Archilla, A. I., Fregenal-Martínez, M. A., Buscalioni, Á. D. & Guerrero, M. C., 2013. Involvement of microbial mats in delayed decay: An experimental essay on fish preservation. *Palaíos*, 28: 56–66.
- Iniesto, M., Buscalioni, Á. D., Guerrero, M. C., Benzerara, K., Moreira, D. & López-Archilla, A. I., 2016. Involvement of microbial mats in early fossilization by decay delay and formation of impressions and replicas of vertebrates and invertebrates. *Scientific Reports*, 6: 1–12.
- Luo, M., Hu, S., Benton, M. J., Shi, G. R., Zhao, L., Huang, J., Song, H., Wen, W., Zhang, Q., Fang, Y., Huang, Y. & Chen, Z. Q., 2017. Taphonomy and palaeobiology of early Middle Triassic coprolites from the Luoping biota, southwest China: Implications for reconstruction of fossil food webs. *Palaeogeography, Palaeoclimatology, Palaeoecology*, 474: 232–246.
- Milán, J., 2012. Crocodylian scatology-A look into morphology, internal architecture, inter-and intraspecific variation and prey remains in extant crocodylian feces. In: Hunt, A. P., Milán, J., Lucas, S. G. & Spielmann, J. A. (eds), *Vertebrate coprolites. New Mexico Museum of Natural History and Science, Bulletin*, 57: 65–72.
- Niedźwiedzki, G., Bajdek, P., Owocki, K. & Kear, B. P., 2016. An Early Triassic polar predator ecosystem revealed by vertebrate coprolites from the Bulgo Sandstone (Sydney Basin) of southeastern Australia. *Palaeogeography, Palaeoclimatology, Palaeoecology*, 464: 5–15.
- Owocki, K., Niedźwiedzki, G., Sennikov, A. G., Golubev, V. K., Janiszewska, K. & Sulej, T., 2012. Upper Permian vertebrate coprolites from the Vyazniki and Gorokhovets, Vyatkian-regional stage, Russian Platform. *Palaíos*, 27: 867–877.
- Penry, D. L. & Jumars, P. A., 1987. Modeling animal guts as chemical reactors. *The American Naturalist*, 129: 69–96.
- Pinto-Lona, A. C. & Andrews, P. J., 1999. Amphibian taphonomy and its implication to the fossil record of Dolina (middle Pleistocene, Atapuerca, Spain). *Palaeogeography, Palaeoclimatology, Palaeoecology*, 149: 411–429.
- Poyato-Ariza, F. J., Talbot, M. R., Fregenal-Martínez, M. A., Meléndez, N. & Wenz, S., 1998. First isotopic and multidisciplinary evidence for nonmarine coelacanths and pycnodontiform fishes: palaeoenvironmental implications. *Palaeogeography, Palaeoclimatology, Palaeoecology*, 144: 65–84.
- Rasband, W. S., 1997–2018. ImageJ, U. S. National Institutes of Health, Bethesda, Maryland, USA. <https://imagej.nih.gov/ij/> (1997-2018).
- Rodríguez-de la Rosa, R. A., Cevallos-Ferriz, S. R. S. & Silva-Pineda, A., 1998. Paleobiological implications of Campanian coprolites. *Palaeogeography, Palaeoclimatology, Palaeoecology*, 142: 231–254.
- Stevens, C. E. & Hume, I. D., 1995. *Comparative Physiology of Vertebrate Digestive System, 2nd Edition*. Cambridge University Press, Cambridge, 400 pp.
- Tappen, M. & Wrangham, R., 2000. Recognizing hominoid-modified bones: the taphonomy of colobus bones partially digested by free-ranging chimpanzees in the Kibale Forest, Uganda. *American Journal of Physical Anthropology*, 113: 217–234.
- Zuschin, M., Harzhauser, M. & Sauermoser, K., 2006. Patchiness of local species richness and its implications for large-scale diversity patterns: an example for the middle Miocene of the Paratethys. *Lethaia*, 39: 65–80.

## Appendix 1

Values of the features used for the non-metric multidimensional scaling (NMDS) analysis.

BHL – bump-headed lace; CIR – circular; CYL – cylinder; CON – cone; ELL – ellipsoidal; ELO – elongated;

FIR – fir-tree; IRR – irregular; ROS – rosary; SPI – spiral; STR – straight lace; TH – thin lace;

NI – number of inclusions (1 <15 ; 2 = 15–30 ; 3 = 31 – 45; 4 >45); PT – pitting (1 – absent; 2 – light; 3 – noticeable; 4 – great); CL–corrosion lines (1 – absent; 2 – slight; 3 – noticeable); CS – chemical signal (1 – light; 2 – moderate; 3 – heavy); DM – diameter in mm (1 < 5; 2 = 5–9.9 ; 3 = 10–19.9; 4 >20); AI – inclusion arrangement (1 – no visible; 2 – fragmented; 3 – articulated; 4 – isolated); FE – shape of the fractures observed at the ends (1 – blunt; 2 – pinched; 3 – straight; 4 – irregular; 5 – all types).

| Specimen | NI | PT | CL | CS | DM | AI | FE |
|----------|----|----|----|----|----|----|----|
| 1BHL     | 4  | 2  | 1  | 1  | 1  | 2  | 5  |
| 2BHL     | 4  | 2  | 2  | 1  | 1  | 2  | 3  |
| 3CIR     | 1  | 2  | 1  | 1  | 1  | 4  | 5  |
| 4CIR     | 3  | 2  | 2  | 1  | 2  | 4  | 5  |
| 5CYL     | 1  | ?  | ?  | ?  | 3  | 1  | ?  |
| 6CYL     | 3  | 2  | 2  | 2  | 2  | 4  | 5  |
| 7CYL     | 1  | ?  | ?  | ?  | 3  | 1  | ?  |
| 8CYL     | 4  | 2  | 1  | 1  | 1  | 4  | 5  |
| 9CON     | 2  | 2  | 2  | 2  | 2  | 4  | 1  |
| 10ELL    | 3  | 2  | 2  | 1  | 1  | 2  | 5  |
| 11ELO    | 2  | 3  | 2  | 2  | 2  | 4  | 1  |
| 12ELO    | 2  | 3  | 2  | 2  | 2  | 4  | 1  |
| 13FIR    | 4  | 2  | 2  | 1  | 1  | 2  | 5  |
| 14IRR    | 1  | ?  | ?  | ?  | 4  | 1  | ?  |
| 15IRR    | 2  | 4  | 2  | 3  | 3  | 2  | 1  |
| 16IRR    | 4  | 2  | 1  | 1  | 1  | 2  | 5  |
| 17ROS    | 4  | 1  | 2  | 1  | 2  | 2  | 4  |
| 18SPI    | 1  | ?  | ?  | ?  | 1  | 4  | ?  |
| 19STR    | 4  | 2  | 2  | 1  | 1  | 2  | 5  |
| 20STR    | 4  | 2  | 1  | 1  | 1  | 2  | 5  |
| 21TH     | 4  | 2  | 1  | 1  | 1  | 2  | 5  |
| 22TH     | 4  | 2  | 2  | 1  | 1  | 2  | 5  |
| 23TH     | 4  | 1  | 2  | 1  | 1  | 2  | 5  |

## Appendix 2

## Detailed description of inclusion characteristics.

**Bump-headed lace coprolites**

- **MCCM-LH15993a** (Fig. 2A–D)
  - **Number of inclusions:** >45.
  - **Inclusions and coprolite size:** Coprolite length is 39.6 mm. Coprolite diameter is about 3.3 mm in the body and 9 mm at the bulge. Inclusions range from 0.2 to 0.9 mm.
  - **Identification of inclusions:** Identified inclusions correspond to the section of a hollow fish vertebra, a plant fragment with parallel fibres, and a possible plant epidermis with a cellular size of about 20 microns. Most of the remains appear fragmented and overlapping.
  - **Action of digestive process:** Inclusions are partially altered with slight pitting. Corrosion lines are absent, and fractures at the ends of inclusions are of all types. The degree of corrosion is light.
- **MCCM-LH35393**
  - **Number of inclusions:** >45.
  - **Inclusions and coprolite size:** Coprolite length is 40 mm. Coprolite diameter is around 3 mm in the body and 9 mm in the bulge. Inclusions usually range from 0.4 to 0.8 mm. Largest inclusions at the bulging end measure 1.3–1.6 mm.
  - **Identification of inclusions:** Identified inclusions correspond to a branchial arch and possible broken fish ribs. Most of the remains appear fragmented and overlapping; occasionally the bigger inclusions appear isolated.
  - **Action of digestive process:** Inclusions are partially altered with slight pitting. Some of the bigger bones present corrosion lines. Fractures at the ends of inclusions are mostly irregular or straight. Some remains are broken and chipped. The degree of corrosion is light.

**Circular coprolites**

- **MCCM-LH21425b**
  - **Number of inclusions:** <15.
  - **Inclusions and coprolite size:** Coprolite length/diameter is around 4.4 mm. Inclusions range from 0.2 to 0.9 mm. The largest inclusion is around 1.6 mm.
  - **Identification of inclusions:** All of them are bony inclusions. The remains appear isolated.
  - **Action of digestive process:** Inclusions are partially altered with slight pitting. Corrosion lines are absent and fractures at the ends of inclusions are of all types. The degree of corrosion is light.
- **MCCM-LH26943b**
  - **Number of inclusions:** 31–45.
  - **Inclusions and coprolite size:** Coprolite length/diameter is around 5.5 mm. Inclusions range from 0.3 to 1.1 mm.
  - **Identification of inclusions:** Identified inclusions correspond to scales. Most of the remains appear isolated.

- **Action of digestive process:** Inclusions are partially altered with slight pitting and some of them exhibit corrosion lines as well. Fractures at the ends of inclusions are of all types. The degree of corrosion is light.

**Cylinder coprolites**

- **MCCM-LH9475A** (Fig. 2E–F)
  - **Number of inclusions:** N <15.
  - **Inclusions and coprolite size:** Coprolite length is 49 mm. Coprolite maximum diameter is 14.5 mm.
  - **Identification of inclusions:** This specimen apparently does not exhibit inclusions on its surface. A small isolated inclusion was identified as being like a sequence of teeth or the internal mould of a tiny, grooved, undetermined fragment, maybe a snail or an arthropod.
  - **Action of digestive process:** Not applicable.
  - Plate ‘b’ is not preserved.
- **MCCM-LH21486B** (Fig. 2G–J)
  - **Number of inclusions:** 31–45.
  - **Inclusions and coprolite size:** Coprolite length is 0.3 mm. Coprolite maximum diameter is 9 mm. Inclusions range from 1.2 to 4.6 mm. A larger inclusion in the middle of the coprolite matrix measures 5.7 mm.
  - **Identification of inclusions:** Four inclusions have been identified as fish scales because of their fusiform shape. The other bony inclusions are isolated in the coprolite matrix.
  - **Action of digestive process:** Fish scales show slight pitting and no corrosion lines; they are probably section cuts of scales. The biggest inclusion presents slight pitting and corrosion lines, with the biggest lines filled with a mineral (probably calcite). The most elongated inclusions show slight pitting over the entire surface and lots of corrosion lines. Fractures at the ends of inclusions are of all types. The degree of corrosion is moderate.
- **MCCM-LH28719A**
  - **Number of inclusions:** N <15.
  - **Inclusions and coprolite size:** Coprolite length is 41.2 mm. Coprolite maximum diameter is 11 mm.
  - **Identification of inclusions:** This specimen apparently does not exhibit inclusions on its surface. In SEM a small and isolated inclusion, perhaps representing bone, was observed.
  - **Action of digestive process:** Not applicable.
  - This specimen is an exception to the common way of naming the fossils. It has a letter at the end of its specimen number, being an isolated coprolite with its dorsal surface exposed.

○ **MCCM-LH-LI15-019**

- **Number of inclusions:** >45.
- **Inclusions and coprolite size:** Coprolite length is 14 mm. Coprolite maximum diameter is 3.8 mm. Inclusions range from 0.2 to 1.1 mm.
- **Identification of inclusions:** Identified inclusions are tubular inclusions (possibly fish ribs) and another one that could be a fish scale in cross-section. Inclusions appear isolated.
- **Action of digestive process:** Some inclusions exhibit slight pitting on their surfaces and an absence of corrosion lines. Fractures at the ends of the inclusions are of all types. The degree of corrosion is light.

**Cone coprolites**

○ **MCCM-LH16609B**

- **Number of inclusions:** 15–30.
- **Inclusions and coprolite size:** Coprolite length is 15.5 mm. Coprolite maximum diameter is around 9 mm. There is a wide inclusion range, from 0.2 to 2.2 mm.
- **Identification of inclusions:** The only identified inclusions are fragments of fish scales and bony pieces. Inclusions appear isolated.
- **Action of digestive process:** The bony tubular inclusions and the fish scales show slight pitting. Bones present corrosion lines on their surface. The deeper lines were produced probably during the rock splitting into part and counterpart. Fractures at the ends of the inclusions are blunt and straight; most of them are covered by coprolite matrix. The degree of corrosion is moderate.

**Ellipsoidal coprolites**

○ **MCCM-LH15929b** (Fig. 2K–M)

- **Number of inclusions:** 30–45.
- **Inclusions and coprolite size:** Coprolite length is 10 mm. Coprolite maximum diameter is 4 mm. Inclusions range from 0.5 to 1.7 mm. The largest inclusion at the edge of the matrix measures 6.8 mm.
- **Identification of inclusions:** Bony inclusions appear both isolated and fragmented. One of the inclusions shows tubercles as ornamentation of a ?ganoid scale, while others exhibit a lamellated bone structure.
- **Action of digestive process:** Most of the inclusions show both slight pitting and slight corrosion lines on their surface. Fractures at the ends of the inclusions are of all types. The degree of corrosion is light.

**Elongated coprolites**

○ **MCCM-LH-LI15-001B** (Fig. 2N–O)

- **Number of inclusions:** 15–30.
- **Inclusions and coprolite size:** Coprolite length is 14.2 mm. Coprolite maximum diameter is 6.6 mm. Inclusions range from 0.7 to 2.9 mm.
- **Identification of inclusions:** Inclusions are bony, isolated fragments, perpendicular to the coprolite matrix.
- **Action of digestive process:** Inclusions present noticeable pitting on their surface, with presence of corrosion lines. Fractures at the ends of the inclusions are both blunt and pinched. The degree of corrosion is moderate.

○ **MCCM-LH-LI15-002A**

- **Number of inclusions:** 15–30.
- **Inclusions and coprolite size:** Coprolite length is 13.2 mm. Coprolite maximum diameter is about 8.3 mm. There is a wide inclusion range that varies from 0.3 to 4.3 mm.
- **Identification of inclusions:** Inclusions are unidentifiable bony remains. Most of them appear isolated.
- **Action of digestive process:** Inclusions present noticeable pitting on their surface, with the presence of slight corrosion lines. Fractures at the ends of the inclusions are mostly blunt. The degree of corrosion is moderate.

**Fir-tree coprolites**

○ **MCCM-LH32378B** (Fig. 3A–B)

- **Number of inclusions:** >45.
- **Inclusions and coprolite size:** Coprolite length is about 9 mm. Coprolite maximum diameter is 4.2 mm. Inclusions range from 0.2 to 1 mm.
- **Identification of inclusions:** The only identified inclusion corresponds to a tooth. The remains appear both isolated and fragmented.
- **Action of digestive process:** Inclusions are partially altered with slight pitting, and some of them exhibit corrosion lines as well. Fractures at the ends of inclusions are of all types. The degree of corrosion is light.

**Irregular coprolites**

○ **MCCM-LH20124**

- **Number of inclusions:** N <15.
- **Inclusions and coprolite size:** Coprolite length is 40 mm. Coprolite maximum diameter is about 26.5 mm.
- **Identification of inclusions:** This specimen apparently does not exhibit inclusions at its surface. At SEM a small and isolated tubular fragment was observed.
- **Action of digestive process:** Not applicable.

○ **MCCM-LH27015A**

- **Number of inclusions:** 15–30.
- **Inclusions and coprolite size:** Coprolite length is around 30 mm. Coprolite maximum diameter is around 12.5 mm. Inclusions range from 0.5 up to 13 mm.
- **Identification of inclusions:** Inclusions are of a bony nature and appear both isolated and fragmented.
- **Action of digestive process:** In longer inclusions, pitting is slight (sometimes absent), but in the wider bony remains deeper holes are observed (great pitting). They show corrosion lines, although perpendicular breakages could have been enhanced by splitting. Most of the ends of inclusions are partially buried in the coprolite matrix, but some blunt ends are observed. The degree of corrosion is heavy.

○ **MCCM-LH28253A** (Fig. 3C–E)

- **Number of inclusions:** >45.
- **Inclusions and coprolite size:** Coprolite length is around 15.5 mm. Coprolite maximum diameter is 4.2 mm. Inclusions range from 0.2 to 0.6 mm.

- **Identification of inclusions:** Identified inclusions are an ostracod valve (?*Cypridea*) and possible, very thin fish vertebrae and ribs. Inclusions appear fragmented.
- **Action of digestive process:** Pitting and corrosion lines are absent. Fractures at the ends of the inclusions are of all types. The degree of corrosion is light.

#### Rosary coprolites

- **MCCM-LH23541A** (Fig. 3F–G)
- **Number of inclusions:** >45.
- **Inclusions and coprolite size:** Coprolite length is around 23 mm. Coprolite maximum diameter is around 5.3 mm. Inclusions range from 0.4 to 2.2 mm.
- **Identification of inclusions:** Identified inclusions are broken ribs, probably from a fish. Inclusions appear fragmented.
- **Action of digestive process:** There is no pitting on the inclusions, just very thin corrosion lines. Fractures at the ends of inclusions are irregular (some inclusions are buried in the coprolite matrix). The degree of corrosion is light.

#### Spiral coprolites

- **MCCM-LH22349**
- **Number of inclusions:** <15.
- **Inclusions and coprolite size:** Coprolite length is 10.4 mm. Coprolite maximum diameter is 4.8 mm. The only two visible inclusions measure 0.3 and 0.5 mm.
- **Identification of inclusions:** Inclusions appear isolated. They are broken and partially covered by the coprolite matrix
- **Action of digestive process:** Not applicable.

#### Straight lace coprolites

- **MCCM-LH16611A**
- **Number of inclusions:** >45.
- **Inclusions and coprolite size:** Coprolite length is around 11.5 mm. Coprolite maximum diameter is around 2 mm. Inclusions range from 0.2 to 0.8 mm.
- **Identification of inclusions:** There is a broken inclusion that could be a vertebra. Inclusions appear fragmented.
- **Action of digestive process:** Some inclusions show both slight pitting and corrosion lines. Fractures at the ends of inclusions are of all types. The degree of corrosion is light.
- **MCCM-LH20198B** (Fig. 3H–J)
- **Number of inclusions:** >45.
- **Inclusions and coprolite size:** Coprolite length is around 28 mm. Coprolite maximum diameter is around 2.8 mm. Inclusions range from 0.2 to 0.8 mm.
- **Identification of inclusions:** Identified inclusions are a transverse section of a fish vertebra with lamellar bone

(wider than the vertebra found in coprolite MCCM-LH15993a), a coalified plant structure, as well as tubular, bony structures (probably ribs). Inclusions appear fragmented.

- **Action of digestive process:** Neither slight pitting nor corrosion lines are observed. Fractures at the ends of the inclusions are of all types. The degree of corrosion is light.
- Plate 'a' is not preserved.

#### Thin lace coprolites

- **MCCM-LH16564A**
- **Number of inclusions:** >45.
- **Inclusions and coprolite size:** Coprolite length is 19.5 mm. Coprolite maximum diameter is around 2 mm. Inclusions range from 0.3 to 1.2 mm.
- **Identification of inclusions:** There are no identifiable inclusions. They appear fragmented.
- **Action of digestive process:** Neither slight pitting nor corrosion lines are observed. Fractures at the ends of the inclusions are of all types. The degree of corrosion is light.

- **MCCM-LH-GQ17-030A** (Fig. 3K–N)
- **Number of inclusions:** >45.
- **Inclusions and coprolite size:** Coprolite length is around 100 mm. Coprolite maximum diameter is around 2.2 mm. Inclusions range from 0.3 to 1.3 mm.
- **Identification of inclusions:** Identified inclusions are several groups of articulated vertebrae, fish rays and ribs. Most of the inclusions appear fragmented and overlapped, and several articulated.
- **Action of digestive process:** Inclusions exhibit both slight pitting and corrosion lines. Fractures at the ends of the inclusions are of all types (sometimes they are buried in the coprolite matrix or under other inclusions). The degree of corrosion is light.
- Plate 'b' is not preserved.

- **MCCM-LH-LI15-028B** (Fig. 3O–Q)
- **Number of inclusions:** >45.
- **Inclusions and coprolite size:** Coprolite length is around 25 mm. Coprolite maximum diameter is around 2.5 mm. Inclusions size ranges from 0.2 to 0.7 mm.
- **Identification of inclusions:** Identified inclusions are vertebrae (some of them seem to be partially articulated and with anchored ribs), possible radius from fins and a palate, which indicates that the possible prey was a macrosemiidid fish (?*Notagogus*) or a juvenile teleost. Most of the inclusions appear fragmented.
- **Action of digestive process:** Inclusions do not show pitting; only some of them show slight corrosion lines. Fractures at the ends of inclusions are of all types. The degree of corrosion is light.

